



JOINT INSTITUTE FOR NUCLEAR RESEARCH

Laboratory of Nuclear Problems

FINAL REPORT ON THE INTEREST PROGRAMME

Study of some aspects of radiation shielding in a preclinical
SPECT/CT scanner prototype using based on Monte Carlo
code systems

Supervisor:

Dr. Antonio Leyva Fabelo

Student:

Alaa ElSadieque

MSc Candidate of Medical Biophysics

Medical Research Institute, Alexandria University

Participation period:

14 February - 25 March, Wave 6

Dubna, 2022

Abstract:

The goal of this work was to become acquainted with a SPECT/CT experimental tomography machine, its biological protection shield, and the calculation of the safe restriction separation that ensures the risk-free operation of this scanner for occupationally exposed employees. The radiation dose distribution in a SPECT/CT scanner prototype was explored using the MCNPX code system for simulation of radiation transport in materials.

Two common sources employed in these devices, as well as various structural combinations, were evaluated in order to identify the shortest path to the core of the apparatus that can be regarded harmless for functionally exposed personnel. The measurements given by the International Commission on Radiological Protection were used as a guideline for assessments.

In all setups, the MCNPX code system was utilized to simulate radiation transmission and examine the dose rate distribution. The radioisotope ^{99m}Tc , with energy of 140 keV, is utilized in SPECT. The dosage rate distribution for different lead wall thicknesses at various distances from the source is displayed, and the findings are studied and explained. The safest distance for our source should be set at 25 cm. The geometry was retained the same for CT, but the source was X-rays from a W anode Roentgen tube. In the case of a 0 cm Pb wall, the safe distance for radiation workers is 7426 cm. The addition of a 0.5 cm Pb wall reduces the safe distance. The percentages of attenuation for both SPECT and CT are also examined.

Introduction:

The number of scientific articles that employ Monte Carlo as a technique of evaluation is increasing, including the estimation of scattering distributions with protection requirements, collimator design, and the influence of changing parameters on image quality [1]. The MC methods are stochastic strategies that analyze problems by using random numbers and probability statistics [2]. Using mathematical models of radiation transport, researchers are able to determine the most optimal and safest radiological conditions under which these systems can be used. Because of this, simulation experiments can be carried out in the most realistic manner possible, and it is possible to calculate with great precision, not only the distribution of doses, but also some hard-to-measure parameters, quickly and economically, using this method [3][4]. Fig.1 showed us the SPECT/CT device during the imaging operation and revealed the quality of image after shooting.

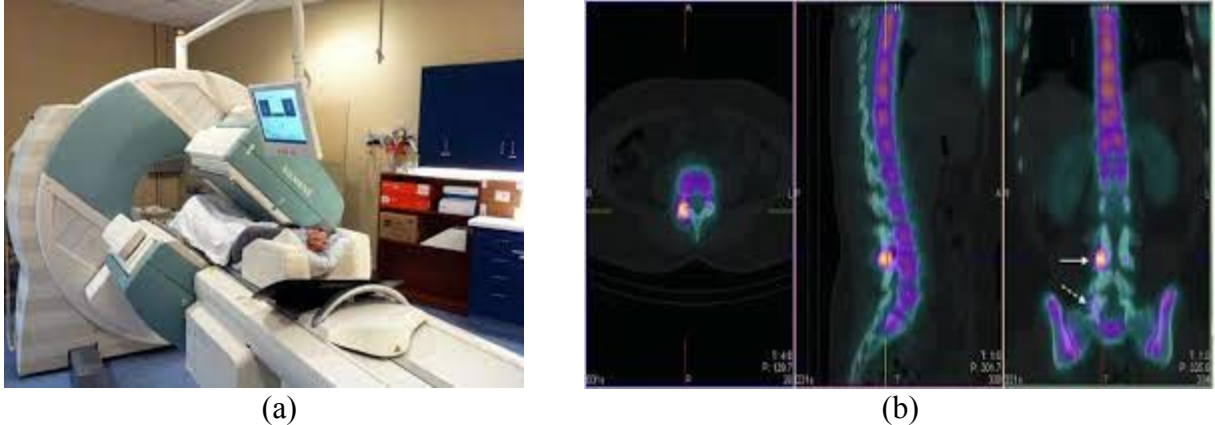


Fig.1. (a) Siemens single-photon emission computed tomography machine in operation, doing a total body bone scan at the Credit Valley Hospital, (b) SPECT/CT images (axial, sagittal, coronal) localizing intense, focal tracer uptake to the right L3/L4 facet joint (continuous arrow). Note is made of mild tracer uptake in the right L5/S1 facet joint (dashed arrow) [5].

The primary goal is to determine the safe working distance for those who are exposed to hazardous conditions at work. MCNPX, a code system based on Monte Carlo method, was used in this case.

Materials and Methods:

- **Computed tomography (CT):**

Computed tomography systems are made up of a front-end, or scanner unit, and a back-end, or control console and viewing station. The X-ray tube, X-ray filter, aperture unit, collimator, detector system, high-voltage generator, cooling system, data-acquisition system (DAS), slip ring, patient table, motors, motor controllers, and mechanical components are all highly developed today.

In the case of the CT, the X-ray emitter rotates around the patient, and the detector, which is placed on the diametrically opposite side, picks up an image of a body section (beam and detector move in synchrony). The computer uses complex mathematical algorithms for image reconstruction to obtain tomographic images of the patient from the data in the "raw" scan. To imagine how high-quality X-ray be produced a modern Philips MRC 600 X-ray tube is shown in Fig. 2a–c. In comparison to conventional ball bearings, a liquid-metal-filled spiral-groove bearing allows for extremely high continuous power. To keep the anode cool, a heat exchanger is frequently placed on the rotating acquisition disc, A schematic of a cone-beam detector system is shown. In contrast to detector systems used in technical CT systems, such as micro-CT (which uses flat-panel detectors), almost all clinical CT systems use cylindrical detector units. The multiarray system forms a cylindrical barrel with the X-ray source at its center, as shown in Fig. 2d. The orientation of the respective X-ray fan inside the cone beam, relative to the axial slice, becomes significant when the number of rows of such multislice detector systems is chosen to be

very high, and the image reconstruction requirements increase. Due to improved spatial resolution and faster image acquisition, modern CT systems are equipped with cone-beam sampling units. In Fig. 2f, a pre assembly, row detector with ribbon cable data is shown. Its 4 194 304 pixels are integrated onto a 41×41 cm² active area [6].

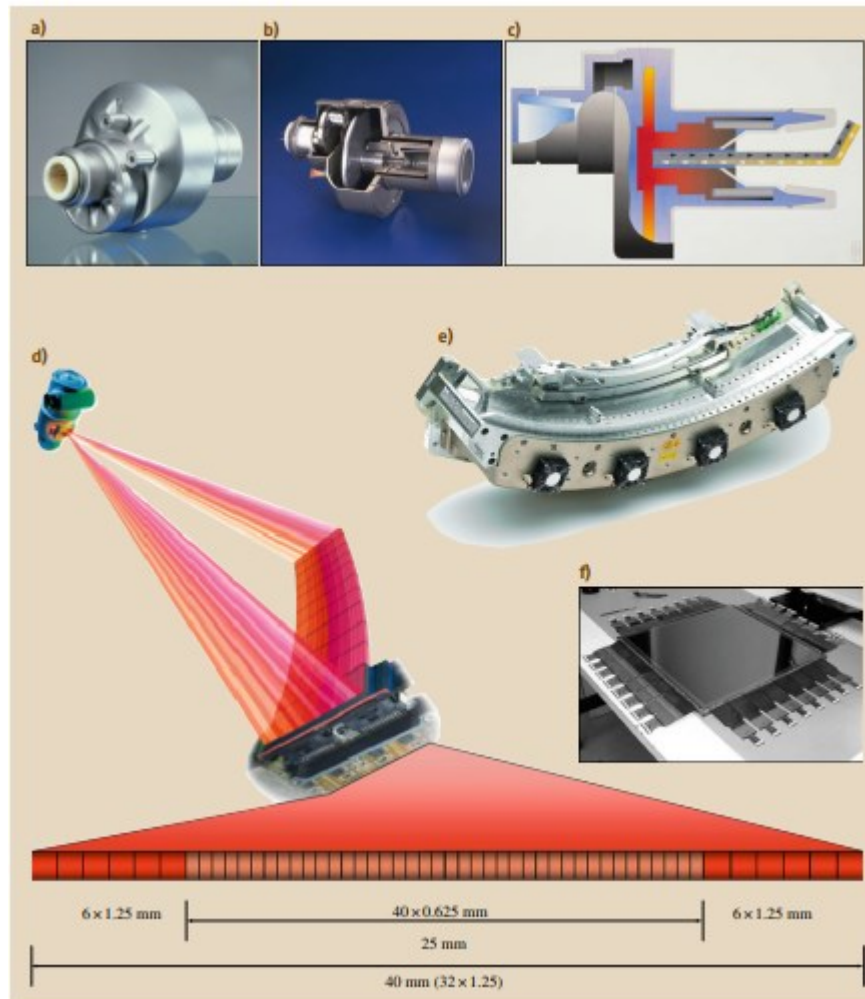


Fig.2. (a,b) Modern high-power X-ray tube and (c) schematic illustration of a modern X-ray tube with a rotating anode disk, (d) schematic illustration of a multislice detector, (e) a detector unit of a 64-row CT system, (f) and the realization of a 41×41 cm² flat-panel detector with 2048×2048 pixels

- **Single photon emission computed tomography (SPECT):**

Specialist can analyze the function of some of your internal organs using a single-photon emission computerized tomography (SPECT) scan. A SPECT scan is a type of nuclear imaging test that creates 3-D images using a radioactive substance and a special camera. While X-rays show what the structures inside your body look like, a SPECT scan produces images that show how your organs function. A SPECT scan, for example, can show how blood flows to your heart or which areas of your brain are more or less active.

Imaging with gamma (γ) rays emitted by radionuclides is very important in nuclear medicine for the detection or staging of a range of diseases such as myocardial perfusion, bone cancer, and thyroid diseases. Single Photon Emission Computed Tomography is a well-known tomographic technique that utilizes a variety of radioisotopes to recreate a emitter's source distribution within a service user. Rapid advances in texture analysis for SPECT systems have been made in recent decades, with a variety of region segmentation techniques to system feedback, photon scattering, and attenuation being developed [7].

- **SPECT-CT tomography:**

Additionally, a SPECT scanner can be used in conjunction with a CT scanner to create hybrid imaging. SPECT/CT is a novel paradigm for obtaining medical and scientific images that enables the acquisition of anatomical information to be combined with functional information.

The SPECT/CT system also includes a patient bed for accurate positioning and computers for the acquisition, reconstruction, and post processing of image data which has been clarified in Fig.3 [8][9].

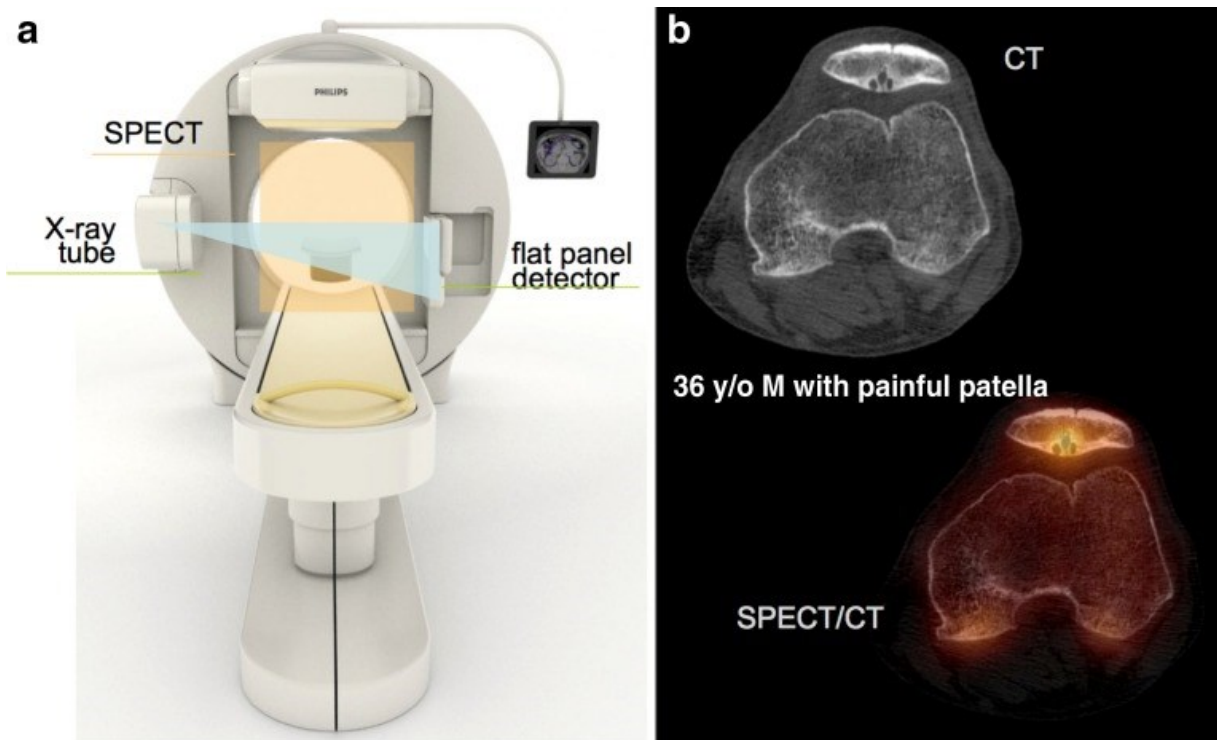


Fig.3 (a) SPECT/CT design with flat panel CT for high-resolution, low-dose CT imaging with a main focus on orthopedic applications (b) and routine attenuation correction.

- **Sources:**

The Roentgen tube is the source of X-rays in CT tomography systems. For the CT configuration, simulations approximated the W anode in the X-ray tube to a point-like source positioned 1 mm in front of a hypothetical tungsten anode. Within a solid angle of 20° , this source emits only in the phantom direction as shown in Fig. 4.

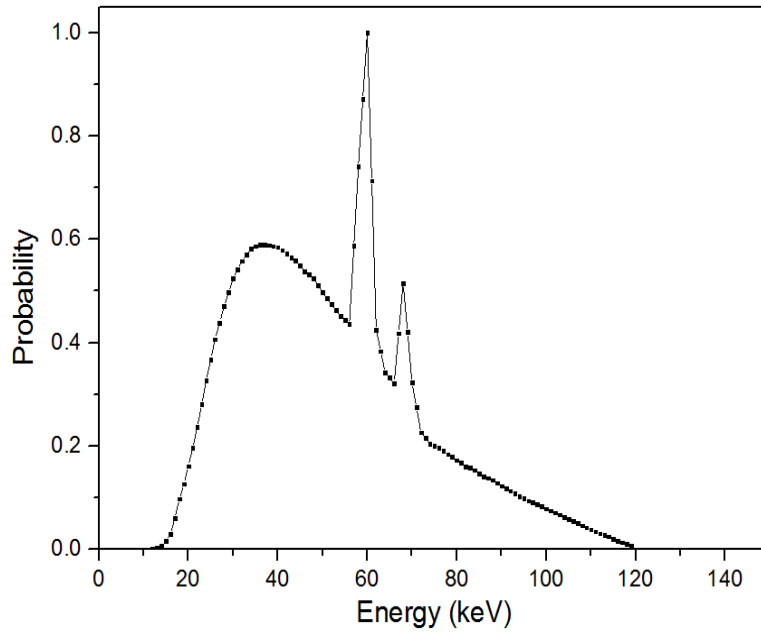


Fig. 4. Tungsten anode spectral model at 1 keV intervals.

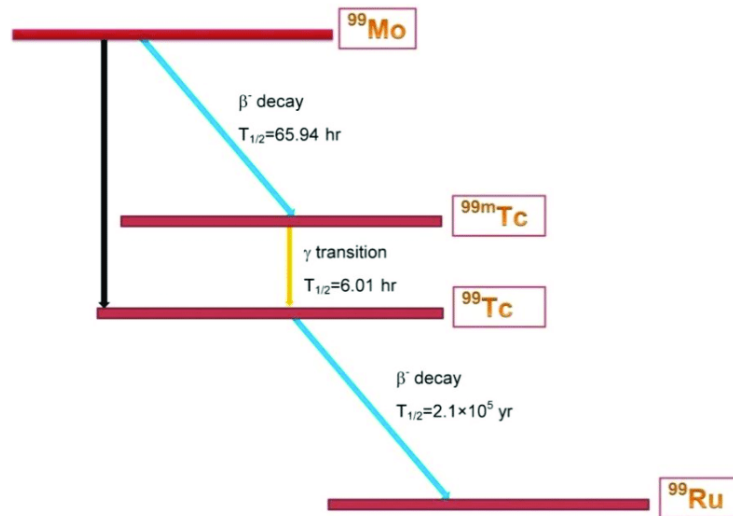


Fig. 5. Decay scheme of ^{99}Mo : The black arrow indicates the transition of ^{99}Mo directly to the ^{99}Tc ground state; blue arrows indicate the transition from ^{99}Mo to $^{99\text{m}}\text{Tc}$ and from ^{99}Tc ground state to ^{99}Ru . The yellow arrow indicates the transition from $^{99\text{m}}\text{Tc}$ to ^{99}Tc .

The gamma radioactive substances source used in the SPECT technique was modeled in simulation as a level source emitting photons isotropically. It is centered on the mouse phantom (coordinate center). The energy of the gamma source is chosen to match the isotope being used, and the activity was measured at 10 MBq. As an illustration, Fig. 5 depicts the decay scheme of ^{99}Mo , the precursor to $^{99\text{m}}\text{Tc}$ [10].

- **Dose limits:**

A whole-body dose rate of 20 mSv/yr, or approximately 2.3 $\mu\text{Sv/hr}$, is considered safe for professionals – those who are exposed to radiation from technical sources and are monitored for dose, such as medical personnel or workers in a nuclear installation who wear personal dosimeters. If only certain parts of the body are exposed, such as the skin, hands, or feet, 500 mSv/yr (57 $\mu\text{Sv/h}$) is still considered safe [11].

Limits are classified into two categories: those that apply to the general public and those that apply to occupationally exposed workers. The ICRP's dose limit for professionals – persons who are exposed to radiation from technical sources and are under dose surveillance, e.g. medical personnel or workers in a nuclear installation wearing a personal dosimeter – a whole-body dose rate of 20 mSv/yr, or about 2.3 $\mu\text{Sv/hr}$, is considered safe. If only parts of the body such as the skin, the hands or the feet are exposed, 500 mSv/yr (57 $\mu\text{Sv/h}$) are still considered safe which can observe in Fig.6 and Table 1.

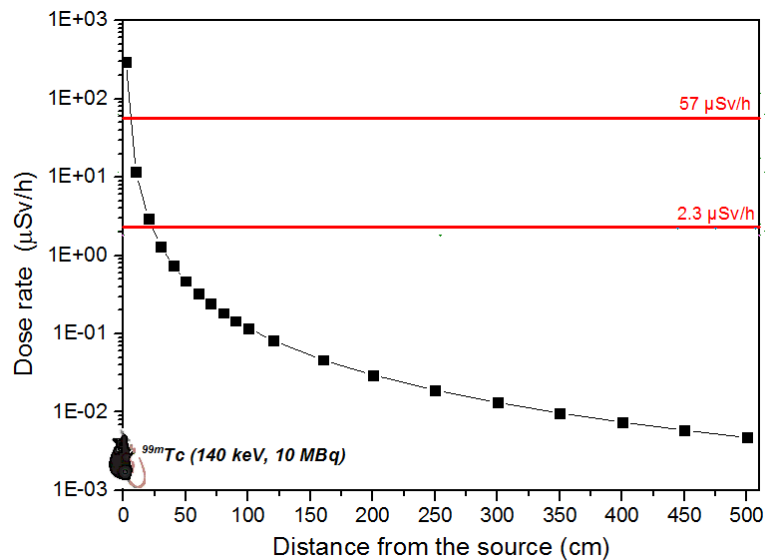


Fig 6. Dose rate ($\mu\text{Sv/h}$) versus distance (cm) from $^{99\text{m}}\text{Tc}$ source in air without wall.

Table 1. Annual Effective Dose

Type of Limit	Occupational Exposure	Exposure to Public
Annual Effective Dose	20 mSv/y averaged over 5y ¹	1 mSv/y
Annual Equivalent Dose: Eye Lens	20 mSv/y averaged over 5y ¹	1 mSv/y
Skin ²	500 mSv	50 mSv
Hands and Feet	500 mSv	50 mSv

There was established as an annual effective dose. As shown in Table 1, an effective dose limit of 20 mSv/year has been established for individuals who perform radiation work.

- **MCNPX:**

MCNPX is a Monte Carlo N-Particle radiation transport code extending the capabilities of MCNP4C [12]. This can be used for neutron, photon, or electron transport, or for neutron/photon/electron transport in combination. Specific application areas include, but are not limited to, radiation protection and dosimetry, radiation shielding, radiography, medical physics, nuclear criticality safety, detector design and analysis, nuclear oil well logging, accelerator target design, fission and fusion reactor design, as well as decontamination and decommissioning. The code handles any three-dimensional material configuration in geometric cells defined by first- and second-degree surfaces and fourth-degree elliptical tori. Pointwise cross-section data are most utilized, but group-wise data are also available. All reactions specified in a specific cross-section evaluation (for example, ENDF/B-VI) are considered for neutrons. Thermal neutrons can be described using either the free gas or S (alpha, beta) models. The code takes into account incoherent and coherent photon scattering, fluorescent emission after photoelectric absorption, absorption in pair production with local emission of annihilation radiation, and bremsstrahlung. A continuous-slowing-down model, which includes positrons, K X-rays, and bremsstrahlung but excludes external or self-induced fields, is used for electron transport. A powerful general source, a criticality source, and a surface source; geometry and output tally plotters; a rich collection of variance reduction techniques; a flexible tally structure; and a large collection of cross-section data are all standard features that contribute to MCNP's versatility and ease of use.

MCNP includes a variety of flexible tallies, such as surface current and flux, volume flux (track length), point or ring detectors, particle heating, fission heating, pulse height tallies for energy or charge deposition, mesh tallies, and radiography tallies. Fig. 7 illustrates how Monte Carlo simulate the performance of (Th_{0.25}U_{0.75})N fuel in a compact nuclear reactor was produced as a case study in order to demonstrate the proof of concept of this fuel form. Neutronic modeling was accomplished through Monte Carlo N-Particle Version 6.2 (MCNP-6); the cross-section of the model is presented in Fig. 7a, and an Abaqus FEA finite element model of a single hexagonal section of the

compact core is shown in Fig. 7b. The basic design requirements are that this core would produce 10 MW (thermal) for 10 years.

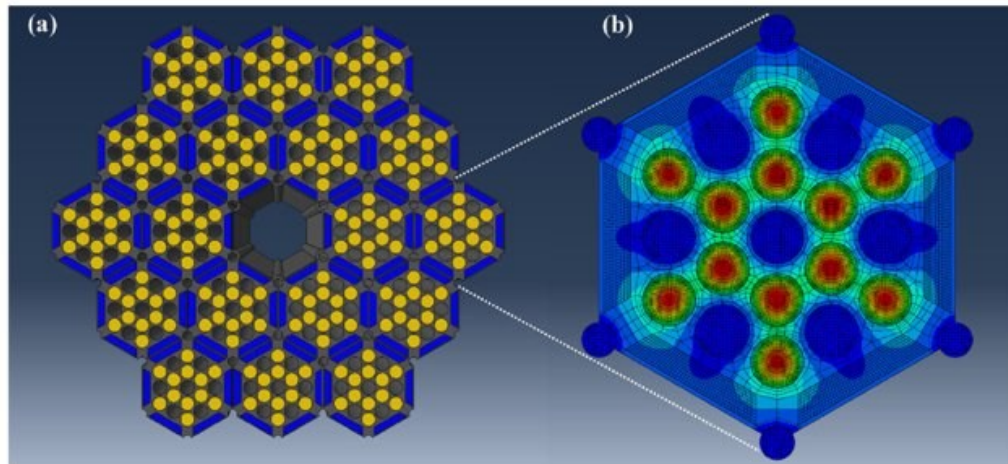


Fig.7. (a) A render of the cross-section of the Monte Carlo N-Particle (MCNP) model of a compact reactor design. Gold zones indicate placement of the mixed (ThxU1À9)N fuel, the gray zone is the primary structural component, and blue zones are the moderator. (b) Given the power deposition calculated by the MCNP model, a finite element model was created for an individual fuel bundle. The colors shown are a heat map: the red zones are the center of the fuel pellets, where the majority of heat is deposited, and the dark blue zones are the coolant channels, which are fixed at 973 K as a boundary condition

Results:

The SPECT technique necessitates the injection of a specific biological molecule that has affinity for the organ or part of the body being studied. This molecule is associated to a radioactive isotope with an indicator function, the radiations of which will be observed by the SPECT system's detectors. Using the MCNPX, determine the dose rate around the scheme and the emission and transport of the gamma radiation emitted by this indicator. To simulate, a group of point detectors were placed at various distances from the source in the MCNPX input file, and the intensity level of particles at those points was recorded with them. The results obtained in cm^{-2} are converted to dose units, pSv, and then to Sv/h. To evaluate the safe transmission distance, these dose rate values are compared to the safe limits established for occupationally exposed workers. The MCNPX code system was used to calculate the dose rate distribution with respect to an animal (laboratory mouse) injected with drug loaded with $^{99\text{m}}\text{Tc}$ (10 MBq activity). The mouse was modelled as a tissue parallelepiped with dimensions of $7 \times 4 \times 4 \text{ cm}^3$ and a density of 1.1 g/cm^3 . The source was positioned in the center of the body model in the center of a cube of muscle tissue (heart) with a density of 1.11 g/cm^3 and dimensions of $0.5 \times 0.5 \times 0.5 \text{ cm}^3$. The particle fluences (cm^{-2}) were calculated using the tally F5 in mode P (photon transport), with the point detector positioned at various distances from

the mouse. The MCNPX's DE and DF cards are used to convert to dose units (Sv) in accordance with ICRP-74.

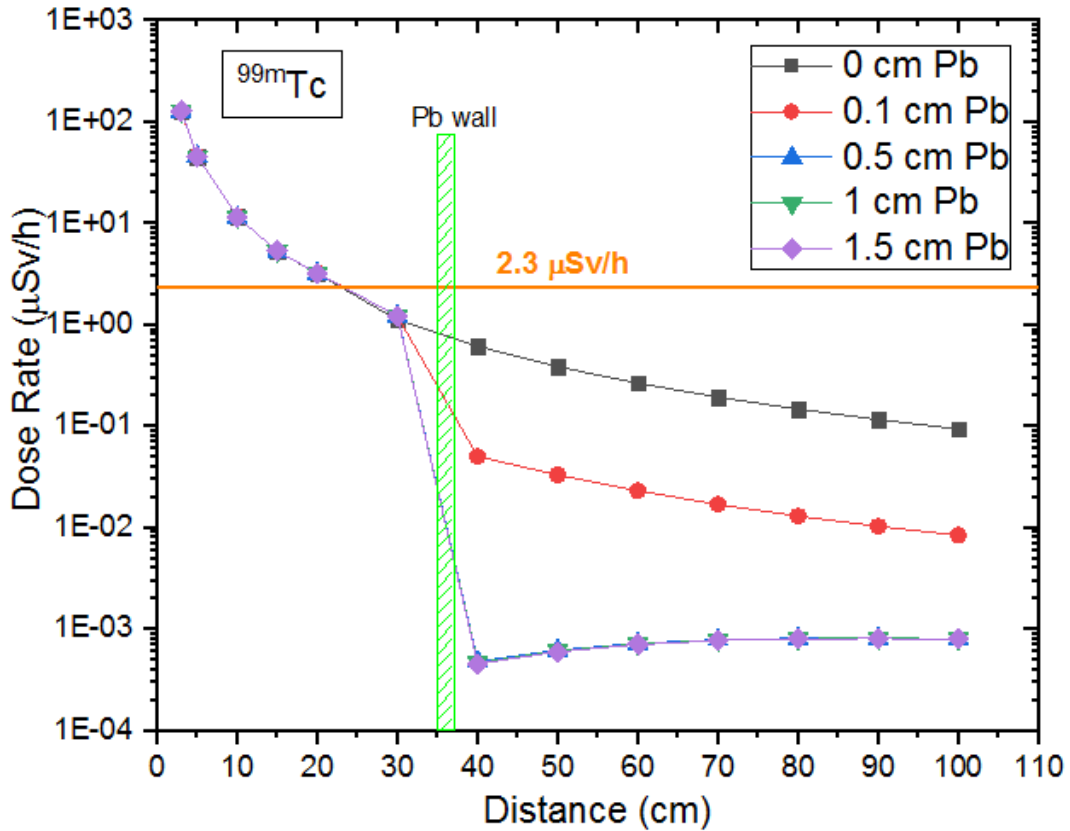


Fig. 8. Dose rate vs. distance behavior calculated for ^{99m}Tc source in five different geometric conditions.

Fig. 8 depicts the results of a dose-rate vs. distance dependence simulation for a ^{99m}Tc source with and without the addition of lead walls of varying thicknesses. A different tape, placed at the correct point in the simulated geometry and of the estimated thickness, identifies the walls inserted in these figure.

Without the lead wall the minimum safe distance is about 25 cm where the dose rate is $2.3\mu\text{Sv}/\text{hrs}$. The thickness of lead wall affected on dose rate which is inversely proportional to the distance far of the radioactive source; so using different lead wall thickness from 0.1 cm to 1.5 cm don't meet the standard dose limits because the resulting dose rate is smaller than the dose limit.

The CT technique was carried out using the same experimental setup as the SPECT simulation, with the exception that an X-ray source with W anode was used instead of the sampling site inside the mouse (-0.05, 0, 0)

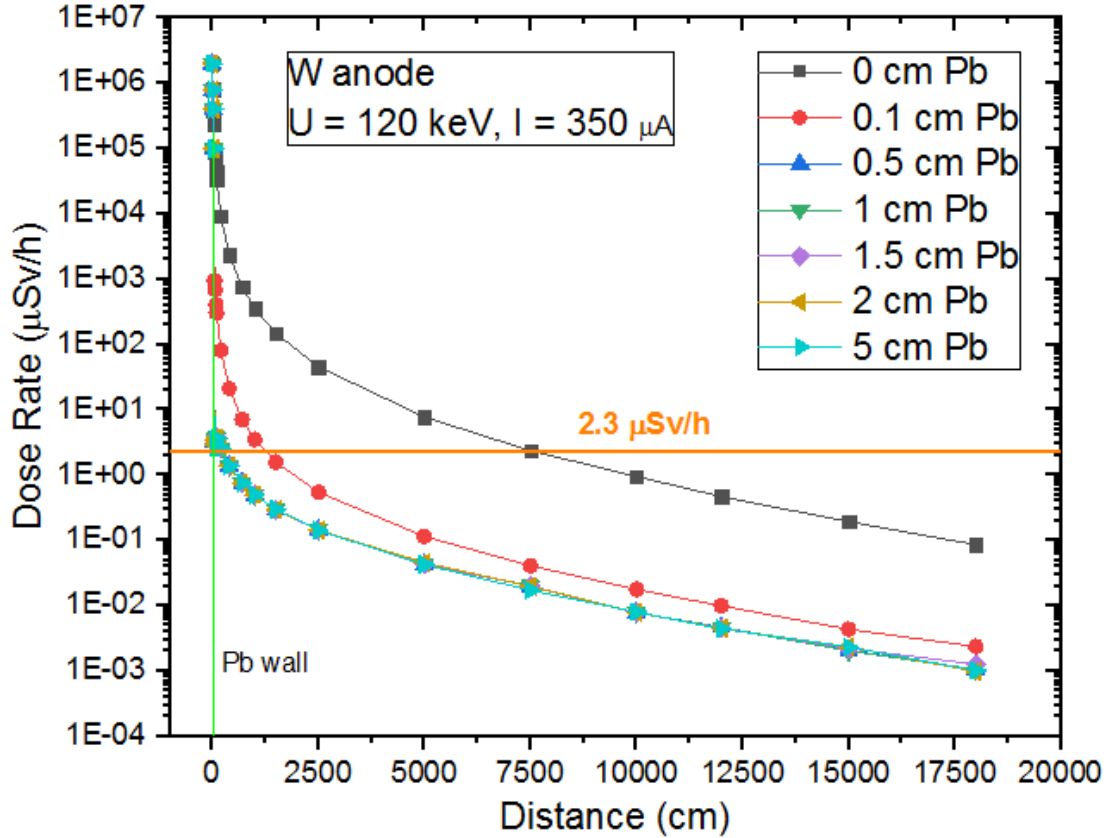


Fig. 9. Dose rate vs distance graph for X-rays.

From Fig. 9, we can see that the minimum safe distance for the limit in 2.3 μ Sv/h is 7608.8 cm.

Using the lead wall with thickness 0.1 cm the safe distance from the radioactive source is 1442 cm to thickness 5 cm is 379 cm that can conclude increasing in lead thickness increase the source attenuation and decrease the safe distance.

Given that the safe distance values determined here for the CT configuration are relatively large, it is justified to use additional means of protection for professionally exposed personnel in addition to the protection provided by the system. Concrete walls, lead bricks, leaded glass, a lead apron, and other additional protective barriers, such as personal protective equipment, are examples.

Conclusion:

Using the MCNPX code system for the simulation of radiation transport in materials, the dose rate distribution has been studied in a SPECT/CT scanner prototype. Two typical sources used in these devices were taken into consideration. The first is the sources of gamma radiation, which are the most common isotopes used in medicine ^{99m}Tc . The second X-ray radiation from the X-ray tube. The goal was to determine for each, the minimum distance to the source that can be considered safe for occupationally exposed personnel. The presence of the arrangement of the protective walls made no considerable differences on the minimum safe distance for source, remaining, 25 cm for ^{99m}Tc . Hence, for this radioisotope, it is possible to construct a simple preclinical SPECT device where no protection walls are considered since the safe distance from the source, for an occupationally exposed worker, is small enough to operate and guarantee his safety without the lead wall. The minimum safe distance when using this isotope without Pb wall protection is equal to 25 cm.

The minimum allowable distance for the skin is small and also does not require additional shielding.

The dose rate vs distance relationship for CT configuration, in absence of any protection wall, showed a minimum safe distance of 7608.8 cm for 2.3 $\mu\text{Sv/h}$. This result revealed that, for the X-rays source studied, there is a maximum thickness value above which increasing this value has no effect on radiation attenuation. This value is 0.5 cm.

Based on the findings, it is clear that 0.5 cm lead protection is required, but it does not provide adequate protection against radiation, particularly X-ray radiation, necessitating the use of alternative methods of protection.

References:

1. Ljungberg, M., Strand, S. E., & King, M. A. (Eds.). (2012). Monte Carlo calculations in nuclear medicine: Applications in diagnostic imaging. CRC Press.
2. Andreo, P. (1991). Monte Carlo techniques in medical radiation physics. *Physics in Medicine & Biology*, 36(7), 861.
3. Rogers, D. W. O. (2006). Fifty years of Monte Carlo simulations for medical physics. *Physics in Medicine & Biology*, 51(13), R287.
4. Lanconelli, N. (2010). The importance of Monte Carlo simulations in modeling detectors for Nuclear Medicine. *Mathematics and Computers in Simulation*, 80(10), 2109-2114.
5. Carstensen, M. H., Al-Harbi, M., Urbain, J. L., & Belhocine, T. Z. (2011). SPECT/CT imaging of the lumbar spine in chronic low back pain: a case report. *Chiropractic & manual therapies*, 19(1), 1-5.

6. Kramme, R., Hoffmann, K. P., & Pozos, R. S. (Eds.). (2011). Springer handbook of medical technology. Springer Science & Business Media.
7. Saib, D. M. A., Azman, N. Z. N., Said, M. A., Aseri, M. I. M., Almarri, H. M., & Ramli, R. M. (2022). Evaluation of butterworth post-filtering effects on contrast and signal noise to ratio values for SPECT images reconstruction. *Radiation Physics and Chemistry*, 192, 109932.
8. Ritt, P. (2022, February). Recent Developments in SPECT/CT. In *Seminars in Nuclear Medicine*. WB Saunders.
9. Beyer, T., Freudenberg, L. S., Townsend, D. W., & Czernin, J. (2011). The future of hybrid imaging—part 1: hybrid imaging technologies and SPECT/CT. *Insights into imaging*, 2(2), 161-169.
10. Capogni, M., Pietropaolo, A., Quintieri, L., Angelone, M., Boschi, A., Capone, M., ... & Pizzuto, A. (2018). 14 MeV neutrons for $^{99}\text{Mo}/^{99\text{m}}\text{Tc}$ production: experiments, simulations and perspectives. *Molecules*, 23(8), 1872.
11. International Commission on Radiological Protection, ICRP-103 The 2007 Recommendations of the International Commission on Radiological Protection, *JAICRP* 37, (2007).
12. Hendricks, J. S. (2003). MCNPX model/table comparison (No. LA--14030). Los Alamos National Lab.

Acknowledgments:

No words can describe my gratitude to the esteemed Professor Antonio and his committed personality. There are no barriers that we faced, but rather the challenges of the language challenge, the challenge of time difference and the challenge of difference in general that we were able to overcome with his guidance and loyalty of the project's supervision role. Thank you, Professor Antonio, and thank you to JINR for being the gateway to knowledge and culture through which we were able to communicate with one of the eminent scientists like Professor Antonio